Study of structural, mechanical, thermal, and electronic structure properties of A_2SnCl_6 (A = Cs, Rb) perovskites for energy generation applications

O. Alsalmi[a,*], M. Rashid[b]
[a]*Physics Department, College of Science, Umm Al-Qura University, P.O. Box 715, Makkah 24382, Saudi Arabia*
[b]*Department of Physics, Jashore University of Science and Technology, Jashore 7408, Bangladesh*

The structural, mechanical, thermal, and electronic structure properties of lead-free vacancy-ordered perovskites A_2SnCl_6 (A = Cs, Rb) were investigated by first-principles calculations under pressure in the DFT framework. DFT is used to study the effect of pressure (0–40 GPa) on these properties of A_2SnCl_6 (A = Cs, Rb) perovskites. The mechanical parameters show that these two perovskites in nature are mechanically stable, anisotropic, and ductile. It is shown that, as pressure increases, the electronic band gap of Cs_2SnCl_6 and Rb_2SnCl_6 increases from 3.495 eV to 4.958 eV and 3.446 eV to 4.722 eV, respectively. Electronic structure calculations show that Sn s orbitals and halogen Cl p orbitals mainly form the conduction band through combination, while the valence band consists only of halogen Cl p orbitals. The mechanical and electronic properties analysis proposes that these two perovskites are potential candidates for optoelectronic applications that work under changing pressure and altitude.

(Received May 20, 2024; Accepted August 7, 2024)

Keywords: A_2SnCl_6 (A = Cs, Rb), Density functional theory (DFT), Lead-free perovskites properties, Pressure effect

1. Introduction

Using materials of high quality and stability is crucial to design efficient devices. Materials scientists have recently become interested in the production of low-cost materials that can function in extreme conditions. Potentially, compounds like perovskites will be critical in this situation [1]. Perovskites have a variety of characteristics, such as conducting, insulating, and semiconducting properties [2]. Also, these materials exhibit outstanding optical, ferroelectric, magnetic, thermoelectric, and charge-ordering features [3-7]. As a result of these properties, perovskite compounds can be used in many applications, including catalyst electrodes, sensors, and solar cells [8].

$APbX_3$ halide perovskites have received considerable interest in the fields of sensitive photodetectors and high-power conversion efficiency because of their exceptional optical and electronic properties [9-11]. Many halide perovskites such as lead-halide perovskites $(PEA)_2PbI_4$, $CsAX_3$ (A = Pb, Sn; X = Cl, Br), Cs_2PbI_4, $CsPbI_2Br$, and $CsPbBr_3$ have been examined with different experimental and theoretical methods [12-18]. Lead perovskites present a serious risk to human health, mental development, and the environment due to their toxicity [19-22]. This problem may be solved by substituting Pb with elements that are less harmful to humans and the environment, including tin (Sn), indium (In), and germanium (Ge) [23-28]. The electronic properties of Sn are comparable to those of Pb, making it a perfect substitution element for Pb within $APbX_3$.

Korbel et al. studied the photovoltaic, piezoelectric, and magnetic properties of compounds made up of ABX_3, in which X is a nonmetallic element and A and B are a wide variety of elements [29]. It was found that 199 stable perovskites exist, of which 71 are new. A screening study using the density functional theory (DFT) method was conducted by Kar and Körzdörfer to identify the most suitable inorganic halide perovskites for solar cell applications [30]. The

* Corresponding author: ohsalmi@uqu.edu.sa
https://doi.org/10.15251/JOR.2024.204.537

researchers found 11 novel perovskites as suitable candidates, including two Cs-based, three K-based, and six Rb-based materials. Tin halide perovskites ($ASnX_3$) possess excellent optoelectronic properties due to long carrier diffusion length and low exciton binding energy [31-34]. For photovoltaic applications, Krishnamoorthy et al. explored the lead-free halide perovskites $AGeI_3$ (A = Cs, CH_3NH_3, $HC(NH_2)_2$) [35]. They discovered that germanium can be used as a replacement for lead in halide perovskite materials with good stability. The DFT method was used by Yunsheng et al. to examine the structural, electrical, and optical properties of $RbSnCl_3$ [36]. Two new phases of Cm and Imm2 were predicted, which have potential for solar energy conversion and other optoelectronic applications. The two phases of $RbSnBr_3$ (cubic and orthorhombic) were studied by Benyahia et al. [37]. They found that in this material, the Br 4P5-to-Sn 5P2 transition has a band gap of 0.57 eV.

Unfortunately, under ambient conditions, $CsSnX_3$ perovskites are relatively unstable since Sn^{2+} can easily oxidize to Sn^{4+} [38,39]. In recent years, many efforts have been directed at resolving the instability problem and commercializing these superior optoelectronic halide perovskites [40-42]. Due to their outstanding properties in many applications, vacancy-ordered double perovskites have attracted the attention of many researchers [43-44].

A vacancy-ordered double perovskite crystal structure is formed by combining two ordinary ABX_3 perovskites, yielding a material that changes from being an insulator to a superconductor [45-49]. Additionally, the natural stability of A_2BX_6 compounds is associated with their shorter bond lengths and stronger bond strengths than ABX_3 compounds [50]. In this regard, the stability of Sn^{4+}-based perovskites (Cs_2SnX_6) is significantly greater than that of Cs_2SnX_6-based perovskites. In the visible and near-infrared (NIR) spectra, Sn-based perovskites exhibit good inferior optical properties compared with Pb-based perovskites [51,52]. In photovoltaic applications, Cs_2SnX_6 perovskites have great potential as light absorbers and hole transporters since they have the advantages of being nontoxic and highly stable under air and moisture exposure [53-59]. It is important for practical optoelectronics applications to understand the structural, mechanical, thermal, and electronic properties of perovskite. The structural properties and stress state of the perovskite layer are major factors affecting the absorption performance of double perovskite solar cells [60]. The bond strength also influences the Debye and melting temperatures. Additionally, matter can be transformed from one phase into another under pressure. However, neither theoretical nor experimental studies have focused enough on the properties of A_2SnCl_6 (A = Cs, Rb) under ambient and pressure-induced conditions. Therefore, for prospective real-life applications, the structural, mechanical, and electronic properties in pressure-induced states need to be reported.

We present a study of lead-free vacancy-ordered perovskites A_2SnCl_6 (A = Cs, Rb) in the ground state and pressure-induced states (up to 40 GPa). The purpose of this study is to cover the gap in information about A_2SnCl_6 (A = Cs, Rb) under pressure and provide the literature with the missing theoretical data regarding these compounds. This will motivate experimental researchers to continue investigating these valuable perovskites for potential energy applications.

There are four sections in this article: Section 1 includes some preliminary information about perovskites and the motivation for working on A_2SnCl_6 (A = Cs, Rb). Section 2 represents the computational method in detail. In Section 3, we show the results of the structural, mechanical, thermal, and electronic properties of the vacancy-ordered perovskites A_2SnCl_6 (A = Cs, Rb) under pressure, along with a discussion of these results. In the last section, a conclusion is drawn to highlight the future potential of this research.

2. Computational methodology

In this work, we investigate the structural, mechanical, thermal, and electronic properties using DFT [61-63] based calculations as implemented in the WIEN2k code [64]. The material is divided into nonoverlapping muffin-tin spheres split by an interstitial space in this method. The exchange−correlation functional in the Kohn−Sham equations is approximated by generalized gradient approximation (GGA) [65]. The basis set convergence is controlled by the cutoff parameter $R_{mt} \times k_{max} = 8.0$, where R_m is the muffin-tin radius (MT) at which the atomic spheres do

not overlap and k_{max} is the largest reciprocal lattice vector. We set l_{max} (angular momentum vector) and G_{max} (Gaussian factor) to 10 and 12, respectively. To validate the accuracy of calculations during the self-consistency cycle (SFC), convergence criteria such as for the energy, force, and charge are set to 0.00001 Ry, 1 mRy/a.u, and 0.0001 e, respectively. For sampling the first Brillouin zone, a mesh of 12 × 12 × 12 k-points is used during the calculation. Additionally, a denser 21 × 21 × 21 k-point mesh is considered to obtain more accurate results in calculating the density of states (DOS).

3. Results and discussion

3.1. Structural properties

The lead-free vacancy-ordered perovskites A_2SnCl_6 (A = Cs, Rb) crystallize into the vacancy-ordered double perovskite structure with space group $Fm\bar{3}m$ (No. 225) (Fig. 1). In Table 1, we show the occupied Wyckoff positions of A_2SnCl_6 (A = Cs, Rb). Fig. 2 shows the optimized energy versus volume curves obtained by fitting the total energy of PBE-GGA to Murnaghan's equation of state (EOS) [66].

$$E(V) = E_0 + \frac{B_0 V}{B_0^{`}}\left[\frac{(V_0/V)^{B_0^{`}}}{B_0^{`}-1}+1\right] - \frac{B_0 V_0}{B_0^{`}-1} \quad (1)$$

The calculated lattice parameters a_0 represented in Table 1 and compared with the available experimental and theoretical data. The calculated lattice parameters are found to be in good agreement with the available data. The lattice parameter decreases in response to the applied pressure. When uniform hydrostatic pressure is applied, the structure remains cubic throughout the calculation process without any phase change.

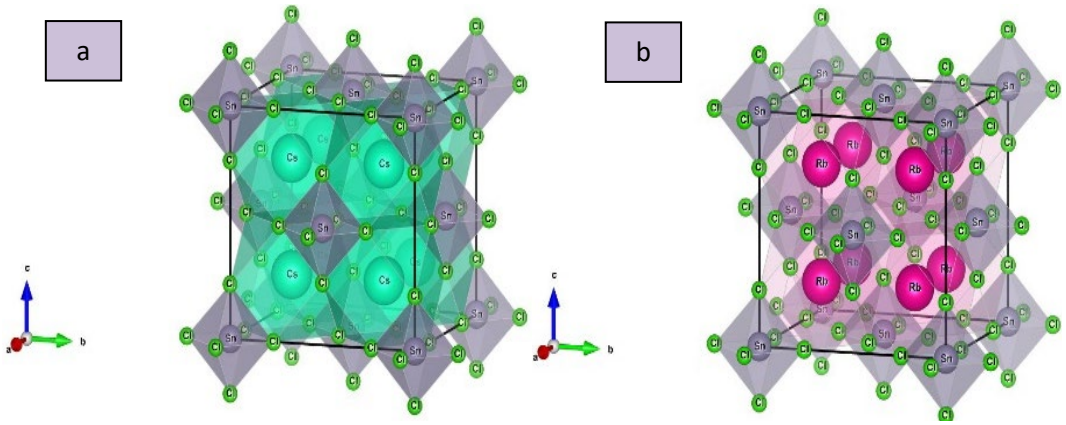

Fig. 1. Crystal structures of the considered metal halide perovskite (a) Cs_2SnCl_6 and (b) Rb_2SnCl_6 compounds.

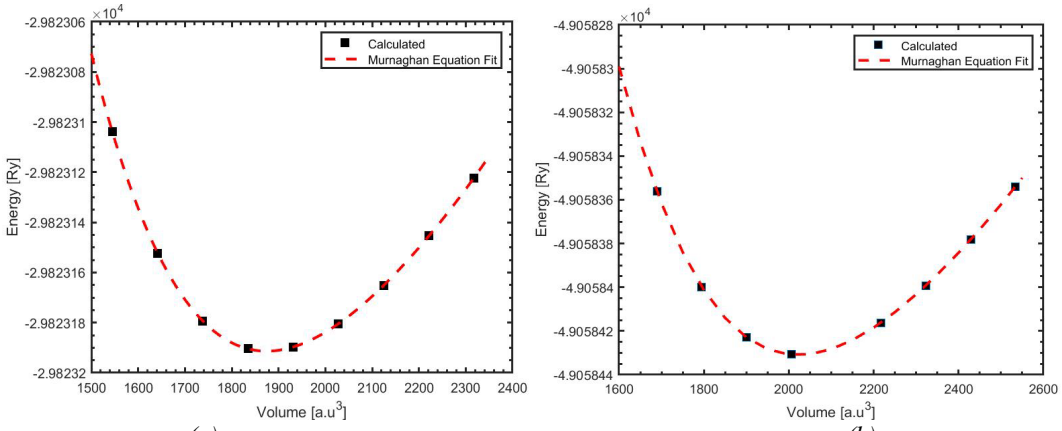

(a) *(b)*

Fig. 2. Energy vs. volume optimization curves for (a) Cs_2SnCl_6 and (b) Rb_2SnCl_6.

Table 1. Optimized lattice constants and Wyckoff positions for Cs_2SnCl_6 and Rb_2SnCl_6 compounds.

Pressure (GPa)	Cs_2SnCl_6	Rb_2SnCl_6	Atom	Wyckoff position		
	Optimized lattice parameter a_0 (Å)			x	y	z
0	10.594 10.367[a] 10.355[b]	10.283 10.137[c] 10.121[d]	Sn 4a	0.0	0.0	0.0
10	10.090	9.858	Cs/ Rb 8c	0.25	0.25	0.25
20	9.799	9.603	Cl 24e	0.245	0.0	0.0
30	9.534	9.375				
40	9.480	9.323				

[a]Ref. [67] [b]Ref. [68] [c]Ref. [69] [d]Ref. [70]

3.2. Mechanical properties

By calculating the elastic constants of crystals, it is possible to predict their mechanical stability. Reliable elastic properties of solid materials can be calculated using first-principle methods. The independent elastic constants (C_{11}, C_{12} and C_{44}) and Cauchy pressure ($C_{cp} = C_{12}$-C_{44}) of the cubic perovskite compounds are calculated by finite strain method [71-74], which are presented in Fig. 3. The elastic constants satisfy the Born stability criteria in equation 2, indicating that these compounds are mechanically stable [75,76].

$$C_{11} - C_{12} > 0, C_{11} + 2C_{12} > 0, C_{44} > 0 \quad (2)$$

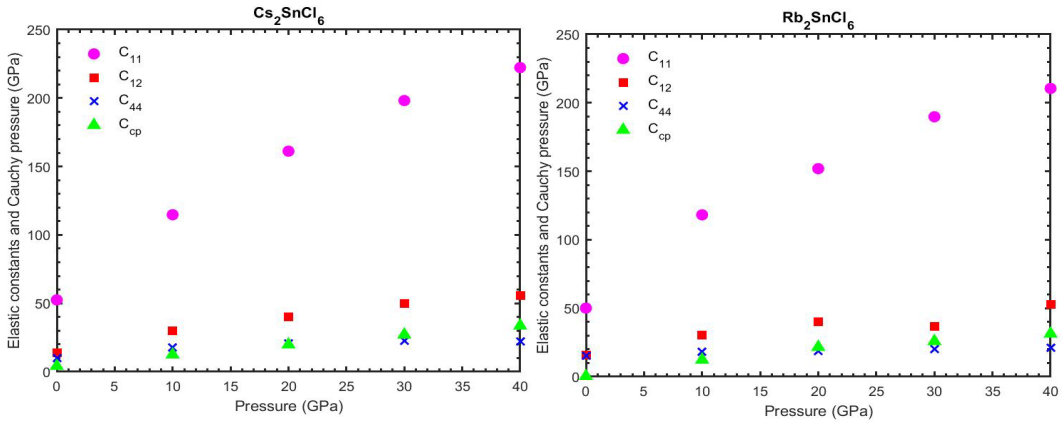

Fig. 3. Variation in elastic constants C_{ij} and Cauchy pressure C_{cp} with pressure for A_2SnCl_6 (A = Cs, Rb).

Table 2. Calculated anisotropy factor A and superplasticity (δ) for A_2SnCl_6 (A = Cs, Rb) compounds.

	Cs_2SnCl_6		Rb_2SnCl_6	
P (GPa)	A	δ	A	δ
0	0.508	19.381	0.884	20.151
10	0.416	39.633	0.412	40.951
20	0.339	52.170	0.333	47.877
30	0.306	61.102	0.309	57.890
40	0.262	64.087	0.270	61.501

An important feature of crystalline solids is elastic anisotropy A. Material that has a significant elastic anisotropy can easily develop microcracks. An in-depth understanding of the mechanical behavior of materials can therefore be gained by analyzing the elastic anisotropy. The Zener anisotropy factor A based on C_{ij} is commonly used to calculate the cubic crystal elastic anisotropy [77]. Additionally, to check the plastic deformation of A_2SnCl_6 (A = Cs, Rb) with pressure, we calculate the superplasticity (δ) [78], which corresponds to the limit of the material at which plastic deformation occurs. Table 2 shows the calculated values of A and δ.

$$A = \frac{2C_{44}}{C_{11} - C_{12}} \tag{3}$$

$$\delta = \frac{1}{C_{11} - C_{12}} \tag{4}$$

Values smaller or larger than one of A indicate elastic anisotropy, while value of one indicate complete elastic isotropy. The level of anisotropy for these two perovskites A_2SnCl_6 (A = Cs, Rb) clearly increases as the pressure increases. In this study, the high values of δ under pressure indicate higher resistance to exhibiting plastic deformation.

Using the elastic constants, some mechanical properties, including the bulk modulus (B), shear modulus (G), Young's modulus (Y), Pugh's ratio (B/G), and Poisson's ratio (v), are also calculated. The variation in these properties with pressure is shown in Fig. 4.

$$B = \frac{C_{11}+2C_{12}}{3} \tag{5}$$

$$\mathrm{G} = \frac{C_{\mathrm{V}}+C_{\mathrm{R}}}{2} \tag{6}$$

$$G_v = \frac{C_{11}-C_{12}+3C_{44}}{5} \tag{7}$$

$$G_R = \frac{5C_{44}(C_{11}-C_{12})}{4C_{44}+3C_{11}-C_{12}} \tag{8}$$

$$Y = \frac{9\mathrm{BG}}{G+3B} \tag{9}$$

$$v = \frac{3B-2G}{2(G+2B)} \tag{10}$$

Under external stress, the material resistance to volume change is determined by its bulk modulus B. Also, it provides insight into the characteristics of the chemical bonds in crystals. As the pressure increases, the bulk modulus B of the A_2SnCl_6 (A = Cs, Rb) compounds increases. Under pressure, chemical bonds become stronger, making these compounds more resistant to volume changes. On the other hand, the shear modulus G indicates the difficulty of changing the shape and microhardness of the material. The shear modulus G of the A_2SnCl_6 (A = Cs, Rb) compounds increases monotonically with increasing pressure. In these compounds, shape changes under external pressure will be more difficult due to the increased microhardness. Solid materials

with a large Young's modulus are stiffer. Young's modulus increases with pressure, indicating that the compounds A_2SnCl_6 (A = Cs, Rb) are more resistant to elastic deformation and highly stiff.

According to Pugh's ratio B/G, solid is considered brittle when this ratio is less than 1.75; otherwise, it is considered ductile. A material that has a higher Pugh's ratio has a higher ductility. Pugh's ratio separates ductile materials from brittle by a critical value of 1.75. The Pugh's ratio for A_2SnCl_6 (A = Cs, Rb) is greater than 1.75; therefore, these perovskites are ductile. The high Pugh's ratios of the A_2SnCl_6 (A = Cs, Rb) perovskites suggest that their ductility makes them suitable for flexible devices. A solid's Poisson's ratio υ gives some insight into the nature of interatomic forces. The central force interactions dominate bonding when Poisson's ratio between 0.25 to 0.50. However, if the ratio falls outside of this range, noncentral forces interactions dominate the force of the solid. The obtained Poisson's ratio υ values for the A_2SnCl_6 (A = Cs, Rb) compounds indicate that the interatomic forces are central interactions in these materials. In addition, Poisson's ratio υ indicates the bonding nature in solids; covalent solids have a value of 0.1, and ionic materials have a value greater than or equal to 0.25 [79]. The A_2SnCl_6 (A = Cs, Rb) compounds have values greater than 0.25, indicating ionic bonding for these compounds.

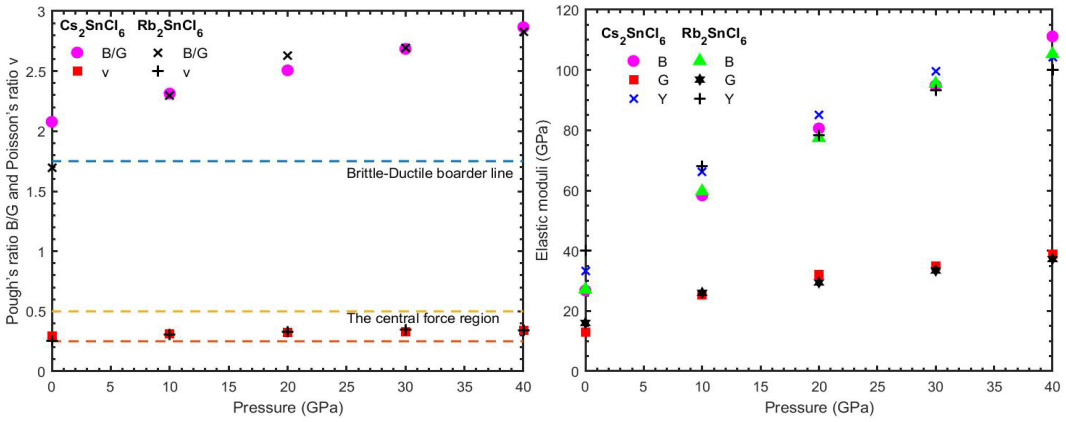

Fig. 4. Variation in the bulk modulus (B), shear modulus (G), Young's modulus (Y), Pugh's ratio and Poisson's ratio with pressure.

3.3. Thermal properties

Debye temperature θ_D is a thermodynamic parameter that is related to elastic constants, bond strength, and melting temperature of materials. Based on the average sound velocity V_m, the Debye temperature is predicted [80].

$$\theta_D = V_m \frac{h}{k_B}\left[\frac{3}{4}\left(\frac{N_A\rho}{M}\right)\right]^{\frac{1}{3}} \tag{11}$$

$$v_l = \sqrt{\left(B + \frac{4}{3}G\right)/\rho} \quad v_s = \sqrt{G/\rho}V_m = \left[\frac{1}{3}\left(\frac{2}{v_s^3} + \frac{1}{v_l^3}\right)\right]^{-\frac{1}{3}}$$

where h, k_B , N_A, ρ, M represent Plank's constant, Boltzmann's constant, Avogadro's number, the density of the solid, and the molecular weight, respectively; v_s and v_l stand for the shear sound velocity and longitudinal sound velocity, respectively.

According to Kumar et al., the Deby temperature and melting temperature of semiconductors in groups II-VI and III-V are linearly related. Solids have a higher melting temperature when their Debye temperature is higher. The following expression can be used to calculate the melting temperature T_m using elastic constant C_{11} [81].

$$T_m = 553\ K + \left(\frac{5.91\ K}{GPa}\right)C_{11} \pm 300K \tag{12}$$

The calculated Debye temperatures and melting temperatures of A_2SnCl_6 (A = Cs, Rb) are listed in Table 3. Obviously, the Debye temperature θ_D increases with pressure. The Debye temperature represents the highest frequency of the lattice vibrations, which shows how strong the bonding between crystal atoms is. Cs_2SnCl_6 has a higher melting temperature than Rb_2SnCl_6, which agrees with the Debye temperature results.

Table 3. Calculated Debye temperature θ_D and melting temperature T_m for A_2SnCl_6 (A = Cs, Rb) compounds.

Pressure (GPa)						
		0	10	20	30	40
θ_D (K)	Cs_2SnCl_6	205.318	278.511	310.438	336.195	336.205
	Rb_2SnCl_6	244.591	281.51	321.016	335.46	356.166
$T_m \pm 300$ (K)	Cs_2SnCl_6	863.227	1231.131	1505.522	1672.68	1866.657
	Rb_2SnCl_6	848.973	1251.501	1450.722	1620.05	1796.856

3.4. Electronic properties

Understanding the electronic structure of materials is important to comprehend their nature at the microscopic level. The electronic properties, including the band structures and density of states (DOS), of A_2SnCl_6 (A = Cs, Rb) compounds under various applied pressures (0−40 GPa) are calculated. Fig. 5 shows the calculated band structures for the first Brillouin zone along the high symmetry points for 0 and 40 GPa pressure. The calculated band structure clearly shows a natural direct band gap at the Γ point, where a valence and conduction band maximum-minimum at the Γ-point, which is suitable for optoelectronic device applications. The band gap values, as obtained with the optimized lattice constants, are listed in Table 4. Pressure-dependent variation of the band gap is shown in Fig. 6. There is an inverse relationship between the lattice constants and the band gap. The band gap increases as the lattice constants decrease because the applied pressure shrinks the lattice dimensions, making the existing states more delocalized, which induces higher repulsive forces. The band structures of A_2SnCl_6 (A = Cs, Rb) indicate a band gap that is consistent with but lower than the experimentally measured band gap. This difference can be explained by the following key factor. A first-principles calculations often underestimate the band gap based on the choice of the exchange correlation functions; the other is the fact that there is difference in lattice constants between theoretical calculations and experimental measurements. However, the band gap increases with decreasing pressure.

To understand the electronic structures in detail, the total density of states (TDOS) and partial density of states (PDOS) of A_2SnCl_6 (A = Cs, Rb) are calculated. Fig. 7 shows the density of states (DOS). The vertical dashed line at 0 eV illustrates the Fermi energy level (E_F); the part above E_F shows the valence band (VB), whereas that below shows the conduction band (CB). These two compounds clearly have very similar electronic structures. The DOS indicates that the VB consists of nonbonding Cl *p* orbitals, whereas the CB is derived from the antibonding states of Sn *s* and Cl *p* orbitals. Under the strong pd hybridization, the band gap increases because more repulsion is applied under pressure. Additionally, the strong hybridization between Sn and Cl plays a critical role in the stability of A_2SnCl_6 (A = Cs, Rb).

Table 4. Calculated band gap E_g (eV) for A_2SnCl_6 (A = Cs, Rb) compounds.

P (GPa)	Cs_2SnCl_6	Rb_2SnCl_6
0	3.495 3.80[a]	3.446 3.85[b]
10	3.691	3.423
20	4.13	3.807
30	4.514	4.147
40	4.958	4.722

[a]Ref. [82] [b]Ref. [70]

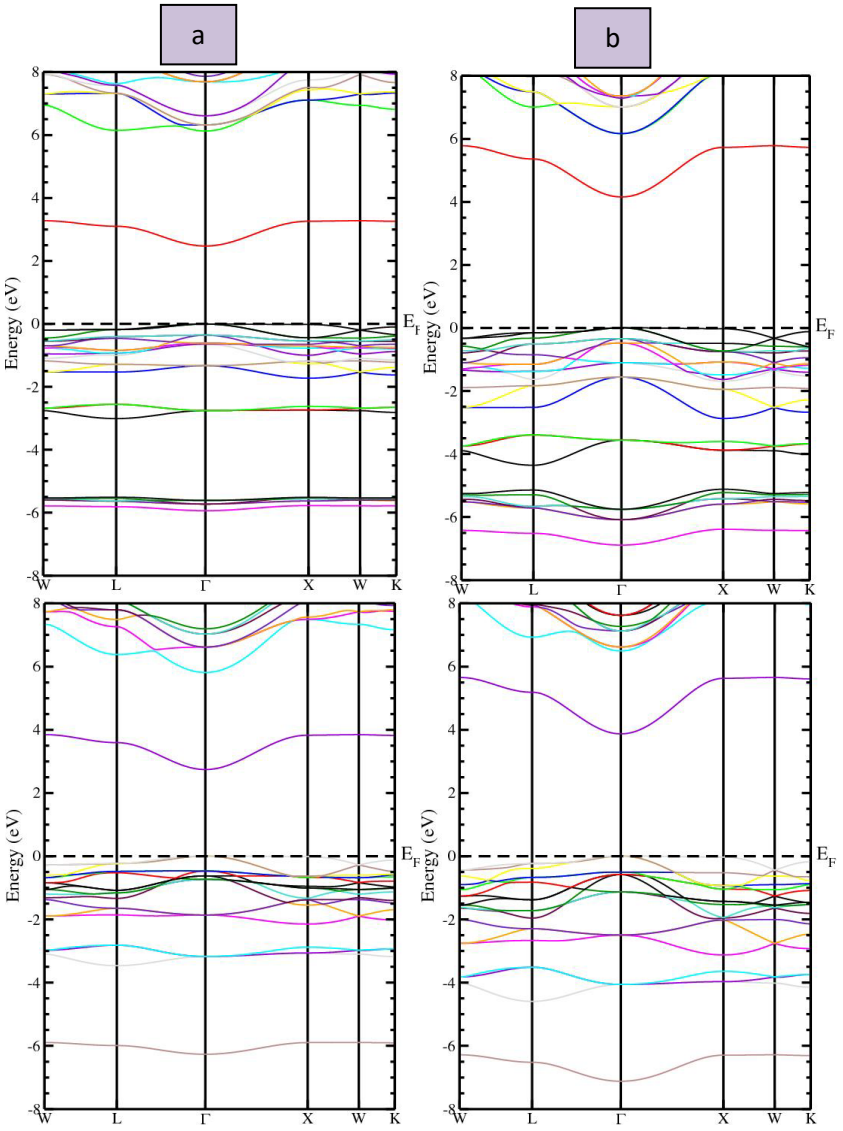

Fig. 5. Band structure plots of (a) Cs_2SnCl_6 and (b) Rb_2SnCl_6 calculated under 0 GPa and 40 GPa pressure.

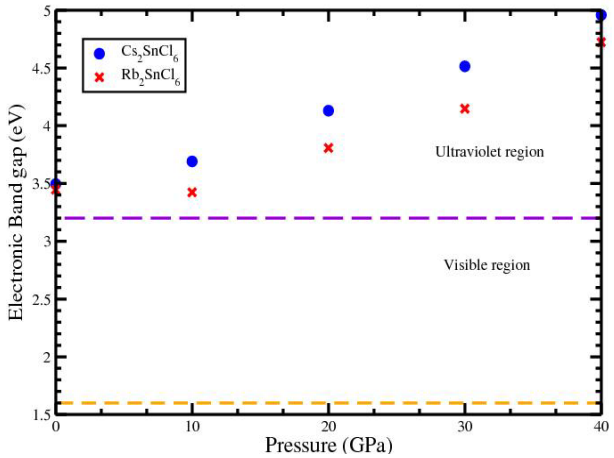

Fig. 6. Band gap variation with pressure from 0 to 40 GPa.

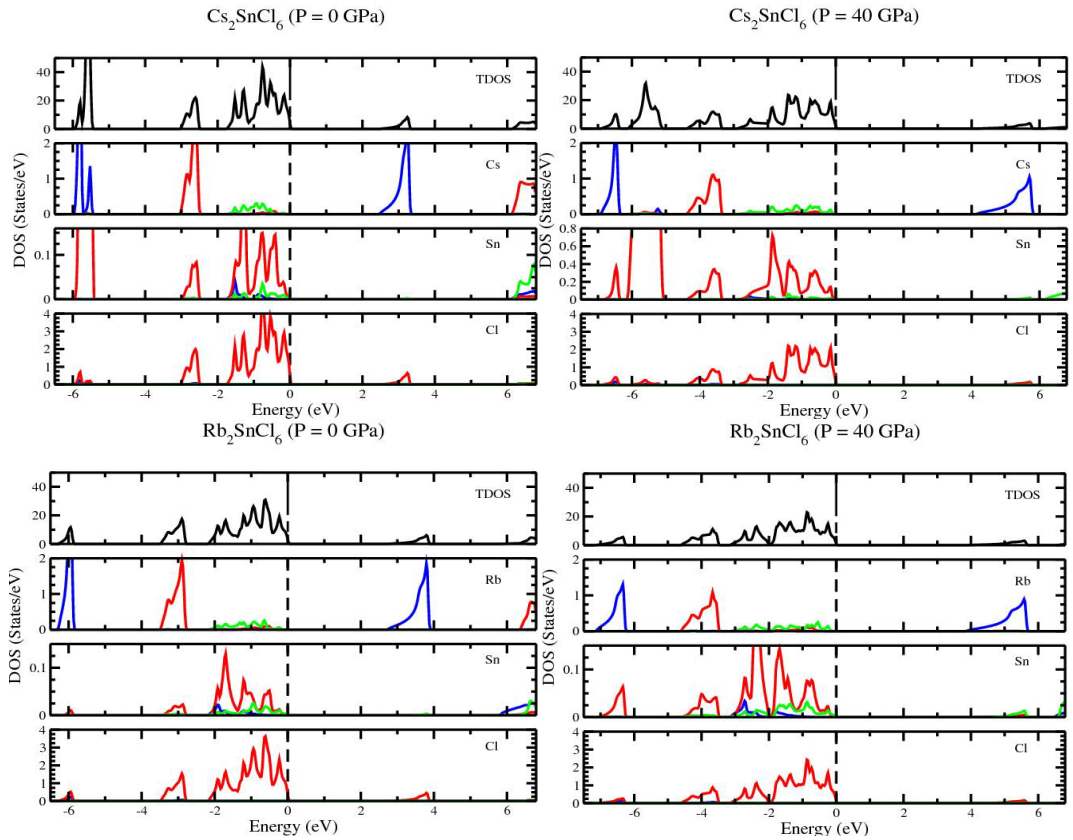

Fig. 7. TDOS and PDOS under applied pressure.

4. Conclusions

In summary, first-principles analysis of the structural, mechanical, thermal, and electronic structures has been performed of the lead-free defect perovskites A_2SnCl_6 (A = Cs, Rb) under pressure using DFT. These calculations are consistent with previously available results, confirming their accuracy. The two compounds are mechanically stable, anisotropic, and ductile. It is found that with increasing pressure, Debye and melting temperatures increase. The electronic band structures show semiconductor characteristics of these compounds, where the band gap increases with increasing pressure. Under the applied pressure, the band structures indicate direct band gaps. According to the DOS, the CB mainly consists of Cl *p* orbitals which hybridized with Sn *s* orbitals, while only the Cl *p* orbitals contribute to the VB. The results indicate that these materials show good properties that allow them to be employed in photovoltaic and optoelectronic devices that operate at various pressures and altitudes.

References

[1] Yan, P., Yang, D., Wang, H., Yang, S., Ge, Z., Energy and Environmental Science, **15**(9), 3630 (2022); https://doi.org/10.1039/D2EE01256A
[2] Senanayak, S.P., Dey, K., Shivanna, R., Li, W., Ghosh, D., Zhang, Y., Roose, B., Zelewski, S. J., Andaji-Garmaroudi, Z., Wood, W., *et al*., Nat. Mater., **22**, 216 (2023); https://doi.org/10.1038/s41563-022-01448-2
[3] Ali, M.A., Ullah, R., Dar, S.A., Murtaza, G., Khan, A., Mahmood, A., Physica Scripta, **95**(7), 075705 (2020); https://doi.org/10.1088/1402-4896/ab8eee
[4] Li, J., Han, Z., Gu, Y., Yu, D., Liu, J., Hu, D., Xu, X., Zeng, H., Advanced Functional Materials, **31**(11), 2008684 (2021); https://doi.org/10.1002/adfm.202008684

[5] Thakur, P., Sharma, N., Pathak, D., Sharma, P., Kishore, K., Dhar, S., Lal, M., Emergent Materials, 1 (2024); https://doi.org/10.1007/s42247-024-00645-w
[6] Maneesha, P., Baral, S. C., Rini, EG. Sen, S., Progress in Solid State Chemistry, 100402 (2023); https://doi.org/10.1016/j.progsolidstchem.2023.100402
[7] Buvaneswaran, S., Shaikh, M., Gowsalya, R., Sahoo, T., Ghosh, S., The Journal of Physical Chemistry C, **127**(31),15486(2023); https://doi.org/10.1021/acs.jpcc.3c02094
[8] Khandy, S. A., Islam, I., Gupta, D. C., Khenata, R., Laref, A., Rubab, S., Materials Research Express, **5**(10), 105702 (2018); https://doi.org/10.1088/2053-1591/aad9eb
[9] Lin, Z., Sun, C., Liu, M., Zeng, R., Liu, M., Fan, Y., Wu, Q., Wei, G., Wang, P., Qiao, Z., Physica Scripta, **99**(2),025921 (2024); https://doi.org/10.1088/1402-4896/ad1967
[10] Simenas, M., Gagor, A., Banys, J., Maczka, M., Chemical Reviews, **124**(5), 2281 (2024); https://doi.org/10.1021/acs.chemrev.3c00532
[11] Han, N. T., Le Manh, T., Dien, V. K., Physica B: Condensed Matter, **682**(0921), 415915 (2024); https://doi.org/10.1016/j.physb.2024.415915
[12] Shan, S., Xu, C., Wu, H., Niu, B., Fu, W., Zuo, L., Chen, H., Advanced Energy Materials, **13**(6), 2203682 (2023); https://doi.org/10.1002/aenm.202203682
[13] Zhao, Yu., Ma, Qi., Liu, B., Yu, Zhuo., Yang, J., Cai, Meng., Nanoscale, **10**(18), 8677 (2018); https://doi.org/10.1039/C8NR00997J
[14] Tong, G., Chen, T., Li, H., Qiu, L., Liu, Z., Dang, Y., Song, W., Ono, L., Jiang, Y., Qi, Y., Nano energy, **65**(2211),1 04015 (2019); https://doi.org/10.1016/j.nanoen.2019.104015
[15] Shukla, A., Sharma, V., Gupta, S., Verma, A., Materials Research Express, **6**(12), 126323 (2020); https://doi.org/10.1088/2053-1591/ab619b
[16] Zhao, Yu., Xu, Y., Zou, Dai., Wang, Jun., Xie, Guo., Liu, B., Cai, Meng., Jiang, Shao., Journal of Physics: Condensed Matter, **32**(19), 195501(2020); https://doi.org/10.1088/1361-648X/ab6d8f
[17] Yan, D. N., Liao, C. S., Zhao, Y. Q., Liu, B., Yang, J. L., Cai, M. Q., Journal of Physics D: Applied Physics, **53**(26), 265302 (2020); https://doi.org/10.1088/1361-6463/ab82d8
[18] Soni, A., Bhamu, K. C., Sahariya, J., Journal of Alloys and Compounds, **817**(0925), 152758 (2020); https://doi.org/10.1016/j.jallcom.2019.152758
[19] Ren, M., Qian, X., Chen, Y., Wang, T., Zhao, Y., Journal of Hazardous Materials, **426**(0304),127848 (2022); https://doi.org/10.1016/j.jhazmat.2021.127848
[20] Babayigit, A., Duy Thanh, D., Ethirajan, A., Manca, J., Muller, M., Boyen, Hans., Conings, B., Scientific reports, **6**(1),18721 (2016); https://doi.org/10.1038/srep18721
[21] Zhu, Y., Kang, Y., Huang, H., Zhuang, D., Li, M., Ling, Z., Peng, K., Zhai, L., Zou, C. Journal of Materials Chemistry A, **12**(5), 2916 (2024); https://doi.org/10.1039/D3TA06303H
[22] Chutia, T., Kalita, T., Kalita, D. J., International Journal of Quantum Chemistry, **124**(1), e27235 (2024); https://doi.org/10.1002/qua.27235
[23] Kalita, T., Chutia, T., Tumung, R., Kalita, D., New Journal of Chemistry, **48**(3)1390 (2024); https://doi.org/10.1039/D3NJ04558G
[24] Men, L., Rosales, B., Gentry, N., Cady, S., Vela, J., ChemNanoMat, **5**(3), 334 (2019); https://doi.org/10.1002/cnma.201800497
[25] Ghosh, B., Wu, B., Mulmudi, H., Guet, C., Weber, K., Sum, T., Mhaisalkar, S., Mathews, N., ACS Applied Materials and Interfaces, **10**(41), 35000 (2018); https://doi.org/10.1021/acsami.7b14735
[26] Han, P., Zhou, W., Zheng, D., Zhang, X., Li, C., Kong, Q., Yang, S., Lu, R., Han, K., Advanced Optical Materials, **10**(1), 2101344 (2022); https://doi.org/10.1002/adom.202101344
[27] Zhang, J., Su, J., Lin, Z., Liu, M., Chang, J., Hao, Y., Applied Physics Letters, **114**(18), (2019); https://doi.org/10.1063/1.5090420
[28] Xing, Y., He, H., Cui, Z., Fu, Z., Qin, S., Zhang, W., Mei, S., Guo, R., Advanced Optical Materials, **12**(13), 2302679 (2024); https://doi.org/10.1002/adom.202302679
[29] Körbel, S., Marques, M. A., Botti, S., Journal of Materials Chemistry C, **4**(15), 3157 (2016); https://doi.org/10.1039/C5TC04172D
[30] Kar, M., Körzdörfer, T., Materials Research Express, **7**(5), 055502 (2020); https://doi.org/10.1088/2053-1591/ab8c0d

[31] Li, D., Xu, W., Zhou, D., Ma, X., Chen, X., Pan, G., Zhu, J., Ji, Y., Ding, N., Song, H., Journal of Luminescence, **216**(0022), 116711(2019); https://doi.org/10.1016/j.jlumin.2019.116711
[32] Liu, Q., Yin, J., Zhang, Bin., Chen, Jia., Zhou, Y., Zhang, Lu., Wang, Lu., Zhao, Q., Hou, J., Shu, J., *et al*., Journal of the American Chemical Society, **143**(14), 5470 (2021);https://doi.org/10.1021/jacs.1c01049
[33] Kang, C., Rao, H., Fang, Y., Zeng, J., Pan, Z., Zhong, X., Angewandte Chemie International Edition, **60**(2), 660 (2021); https://doi.org/10.1002/anie.202011569
[34] Roknuzzaman, M., Ostrikov, K., Wasalathilake, K., Yan, C., Wang, H., Tesfamichael, T., Organic Electronics, **59**(1566), 99 (2018); https://doi.org/10.1016/j.orgel.2018.04.051
[35] Krishnamoorthy, T., Ding, H., Yan, C., Leong, W., Baikie, T., Zhang, Z., Sherburne, M., Li, S., Asta, M., Mathews, N., *et al*., Journal of Materials Chemistry A, **3**(47), 23829 (2015);https://doi.org/10.1039/C5TA05741H
[36] Li, Y., Gong, X., Zhang, P., Shao, X., Chemical Physics Letters, **716**(0009), 76 (2019); https://doi.org/10.1016/j.cplett.2018.12.011
[37] Khan, K., Sahariya, J., Soni, A., Materials Chemistry and Physics, **262**(0254), 124284 (2021); https://doi.org/10.1016/j.matchemphys.2021.124284
[38] Chen, Y. J., Hou, C., Yang, Y., Physical Chemistry Chemical Physics, **25**(15), 10583(2023); https://doi.org/10.1039/D2CP04183A
[39] Wang, T., Yan, F., Chemistry An Asian Journal, **15**(10), 1524 (2020); https://doi.org/10.1002/asia.202000160
[40] Rolston, N., Bush, K., Printz, A., Gold-Parker, A., Ding, Y., Toney, M., McGehee, M., Dauskardt, R., Advanced Energy Materials, **8**(29), 1802139 (2018); https://doi.org/10.1002/aenm.201802139
[41] Bai, S., Da, P., Li, C., Wang, Z., Yuan, Z., Fu, F., Kawecki, M., Liu, X., Sakai, N., Wang, J., *et al*., Nature, **571**(7764), 245 (2019); https://doi.org/10.1038/s41586-019-1357-2
[42] Wu, Wu., Yang, Z., Rudd, P., Shao, Y., Dai, X., Wei, H., Zhao, J., Fang, Y., Wang, Q., Liu, Y., Science advances, **5**(3), eaav8925 (2019); https://doi.org/10.1126/sciadv.aav8925
[43] Yadav, A., Mansoorie, F. N., Saini, A., Bag, M., ACS Sustainable Chemistry and Engineering, **12**(2), 1029 (2024); https://doi.org/10.1021/acssuschemeng.3c06645
[44] Nipa, N. A., Afridi, A. M., Rashid, M. A., Computational and Theoretical Chemistry, **1235**(2210), 114572 (2024); https://doi.org/10.1016/j.comptc.2024.114572
[45] Ghorui, S., Kangsabanik, J., Aslam, M., Alam, A., Physical Review Applied, **21**(2), 024036 (2024); https://doi.org/10.1103/PhysRevApplied.21.024036
[46] Zikem, A., Baaziz, H., Ghellab, T., Charifi, Z., Soyalp, F., Physica Scripta, **99**(3), 035917 (2024); https://doi.org/10.1088/1402-4896/ad1ad8
[47] Liu, Y., Zhou, J., Guan, Y., Xiao, Y., Dong, H., Wu, F., Huang, L., Applied Physics Letters, **124**(4), 042105 (2024); https://doi.org/10.1063/5.0179731
[48] Rehman, M. U., Wang, Q., Yu, Y., Crystals, **12**(11), 1597 (2022); https://doi.org/10.3390/cryst12111597
[49] Pal, B., Kale, A. J., Sharma, M., Bhamu, K. C., Kang, S. G., Singh, V. K., Dixit, A., Energy and Fuels, **38**(2), 1430 (2024); https://doi.org/10.1021/acs.energyfuels.3c03030
[50] Chu, Y., Hu, Y., Xiao, Z., The Journal of Physical Chemistry C, **125**(18), 9688 (2021); https://doi.org/10.1021/acs.jpcc.1c02312
[51] Zhang, X., Wu, X., Liu, X., Chen, G., Wang, Y., Bao, J., Xu, X., Liu, X., Zhang, Q., Yu, K., *et al*., Journal of the American Chemical Society, **142**(9), 4464 (2020);https://doi.org/10.1021/jacs.9b13681
[52] Zeng, M., Locardi, F., Mara, D., Hens, Z., Van Deun, R., Artizzu, F., Nanoscale, **13**(17), 8118 (2021); https://doi.org/10.1039/D1NR00385B
[53] Lin, H., Li, S., Zhang, Y., Chu, C., MacSwain, W., Meulenberg, R., Qiao, Q., Zhao, D., Zheng, W., Advanced Functional Materials, **34**(7), 2309480 (2024); https://doi.org/10.1002/adfm.202309480
[54] Ke, J. C. R., Lewis, D. J., Walton, A. S., Spencer, B. F., O'Brien, P., Thomas, A. G., Flavell, W. R., Journal of Materials Chemistry A, **6**(24), 11205 (2018); https://doi.org/10.1039/C8TA03133A

[55] Khuili, M., Ouhammou, A., Fazouan, N., Atmani, EH., Allaoui, I., Al-Qaisi, S., Maher, K., Bouidmar, R., Modern Physics Letters B, **38**(01), 2350223 (2024); https://doi.org/10.1142/S0217984923502238
[56] Cheng, R., Zeng, Z., Wang, C., Ouyang, N., Chen, Y., Physical Review B, **109**(5), 054305 (2024); https://doi.org/10.1103/PhysRevB.109.054305
[57] Hoang, M. H., Le, M. D., Le Anh, T., Nguyen, Q. K., DO, T. A. T., Ho, T. G., Man, M. T., Journal of Physics: Condensed Matter, **36**(28), 285901 (2024). https://doi.org/10.1088/1361-648X/ad3ac4
[58] Geng, M., Pan, X., Zhao, J., Wang, X., Liu, R., Xu, Z., Ma, N., Gao, M., Shao, M., Li, J., Chemical Engineering Journal, **486**(1385), 150222 (2024); https://doi.org/10.1016/j.cej.2024.150222
[59] Han, X., Liang, J., Yang, Ji., Soni, K., Fang, Q., Wang, W., Zhang, J., Jia, S., Mart, A., Zhao, Y., *et al*., Small, **15**(39), 1901650 (2019); https://doi.org/10.1002/smll.201901650
[60] Dong, Q., Chen, M., Liu, Y., Eickemeyer, F., Zhao, W., Dai, Z., Yin, Y., Jiang, C., Feng, J., Jin, S., *et al*., Joule, **5**(6)1587 (2021); https://doi.org/10.1016/j.joule.2021.04.014
[61] Hohenberg, P., Kohn, W., Phys. Rev., **136**(3B), B864 (1964); https://doi.org/10.1103/PhysRev.136.B864
[62] Kohn, W., Sham, L. J., Physical Review, **140**(4A). A1133 (1965); https://doi.org/10.1103/PhysRev.140.A1133
[63] Kohn, W., Sham, L. J., Physical Review, **137**(6A), A1697 (1965); https://doi.org/10.1103/PhysRev.137.A1697
[64] P. Blaha, K. Schwarz, G.K.H. Madsen, D. Kvasnicka, J. Luitz, WIEN2k, An Augmented Plane Wave Plus Local Orbitals Program for Calculating Crystal Properties (Vienna University of Technology, Vienna Austria, 2001).
[65] Perdew, J. P., Burke, K., Ernzerhof, M., Physical review letters, **77**(18), 3865 (1996); https://doi.org/10.1103/PhysRevLett.77.3865
[66] Murnaghan, F. D., Proceedings of the National Academy of Sciences, **30**(9), 244 (1944); https://doi.org/10.1073/pnas.30.9.24
[67] Brik, M. G., Kityk, I. V., Journal of Physics and Chemistry of Solids, **72**(11), 1256 (2011); https://doi.org/10.1016/j.jpcs.2011.07.016
[68] Brill, T. B., Gearhart, R. C., Welsh, W. A., Journal of Magnetic Resonance (1969), **13**(1), 27 (1974); https://doi.org/10.1016/0022-2364(74)90101-2
[69] Abriel, W., Zehnder, E. J., Zeitschrift für Naturforschung B, **42**(10), 1273 (1987); https://doi.org/10.1515/znb-1987-1012
[70] Qamar, S. A., Lin, T. W., Tsai, Y. T., Lin, C. C., ACS Applied Nano Materials, **5**(5), 7580 (2022); https://doi.org/10.1021/acsanm.2c01647
[71] Murnaghan, F. D., American Journal of Mathematics, **59**(2), 235 (1937); https://doi.org/10.2307/2371405
[72] Hershey, A., J. Appl. Mech., **21**(3), 236 (1954); https://doi.org/10.1115/1.4010899
[73] Kröner, E., Zeitschrift für Physik, **151**(4), 504 (1958); https://doi.org/10.1007/BF01337948
[74] Mehl, M. J., Osburn, J. E., Papaconstantopoulos, D. A., Klein, B. M., Physical Review B, **41**(15), 10311 (1990); https://doi.org/10.1103/PhysRevB.41.10311
[75] Born, M., Cambridge University Press. P, **36**(2), 160 (1940); https://doi.org/10.1017/S0305004100017138
[76] Hill, R., Cambridge University Press. P, **77**(1), 225 (1975); https://doi.org/10.1017/S0305004100049549
[77] Zener, C. M., Siegel, S., The Journal of Physical Chemistry, **53**(9), 1468 (1949); https://doi.org/10.1021/j150474a017
[78] Souvatzis, P., Katsnelson, M. I., Simak, S., Ahuja, R., Eriksson, O., Mohn, P., Physical Review B, **70**(1), 012201 (2004); https://doi.org/10.1103/PhysRevB.70.012201
[79] ŠIMŮNEK, A., Physical Review B, **75**(17), 172108 (2007); https://doi.org/10.1103/PhysRevB.75.172108
[80] Anderson, O. L., Journal of Physics and Chemistry of Solids, **24**(7), 909 (1963); https://doi.org/10.1016/0022-3697(63)90067-2

[81] Fine, M. E., Brown, L. D., Marcus, H. L., Scripta metallurgica, **18**(9), 951 (1984); https://doi.org/10.1016/0036-9748(84)90267-9
[82] Bhat, A. A., Khandy, S. A., Ali, A. M., Tomar, R., The Journal of Physical Chemistry Letters, **14**(21), 5004 (2023); https://doi.org/10.1021/acs.jpclett.3c00522